Solid-State Electronics, 1972, Vol. 15, pp. 145–158. Pergamon Press. Printed in Great Britain

MODELS FOR CONTACTS TO PLANAR DEVICES*

H. H. BERGER
IBM Laboratories, D/3197, Schoenaicher Strasse 220, Boeblingen, Germany

(*Received* 22 *March* 1971; *in revised form* 23 *June* 1971)

Abstract—Two basic models for rectangular contacts to planar devices, the Kennedy–Murley Model (KMM)[1] and the Transmission Line Model (TLM)[2, 3] are discussed and compared. The KMM does not take into account the interface resistance between metal and semiconductor, whereas the TLM disregards the vertical structure of the semiconductor layer. An extension of the TLM is derived (ETLM), which approximately considers this vertical structure. KMM and TLM thus appear as special cases of the ETLM. The calibration of the latter on the KMM then yields a simple quantitative criterion for the applicability of the KMM or the pure TLM. Measurement results on typical aluminum–silicon contacts are described satisfactorily by the (E)TLM. Concurrently with the applicability criterion, the KMM proves inadequate for these contacts due to the disregard of interface resistance. Conclusions are derived from the TLM pertaining to current distribution over the contact area and to contact resistance. In particular, the contacts are classified according to their operation mode. Finally, the TLM approach is applied also to circular contacts.

NOTATION

Rationalized MKSA units are used

- A_c contact area
- C constant used in the ETLM
- C' capacitance per unit length
- C^* capacitance per unit area
- d contact length
- f frequency
- G' line shunt conductance per unit length
- $\underline{G}'$ complex line shunt admittance per unit length
- h thickness of semiconductor layer
- $\underline{I}$ complex current
- i current (d.c.)
- $\mathscr{j}$ $\sqrt{(-1)}$
- j current density
- $\hat{j}$ peak current density
- $\bar{j}$ average current density
- k end correction for resistor calculation
- L diffusion length of dopant atoms
- l distance between two contacts on a resistor
- R' line resistance per unit length
- R_c contact resistance
- R_{ci} contact resistance of an intermediate contact
- R_{ct} contact resistance of a terminal contact
- R_{cv} contact resistance of a vertical type contact
- R_e contact end resistance
- R_l lateral crowding resistance of a rectangular contact ($w < W$)
- R_s sheet resistance of a resistive layer
- R_{ss} total series resistance of the semiconductor layer beneath the contact
- r radius; variable distance from a center point
- r_d radius of a circular contact
- v voltage (d.c.)
- $\underline{V}$ complex voltage
- W resistor width
- w contact width
- x variable distance from the leading contact edge
- Z characteristic line resistance
- $\underline{Z}$ complex characteristic line impedance
- Z^* characteristic resistance in the ETLM
- α attenuation constant of a transmission line (α_0 = d.c. value, α^* for ETLM)
- β phase constant of a transmission line
- γ propagation constant of a transmission line ($= \alpha + j\beta$)
- δ distance between resistor edge and contact edge
- η ratio of vertical resistances of interface and semiconductor layer per unit area
- ρ_c contact resistivity (Ω cm^2)
- ρ_c^* apparent contact resistivity
- ρ_B resistivity of a homogeneous semiconductor layer (Ω cm)
- Ω normalized frequency
- ω $2 \cdot \pi \cdot f$

1. INTRODUCTION

THE OHMIC contacts to planar devices are of great importance in the quality and reliability of monolithic circuits. Hence, these contacts† need a thorough analysis, especially in view of the ever increasing component densities in monolithic structures.

The first published attempt to describe the typical planar contacts of such monolithic struc-

*This paper comprises parts of a doctoral thesis approved by the faculty of electrical engineering of the Technische Hochschule Aachen/Germany.

†In the following these contacts to planar devices shall be shortly referred to as 'planar contacts'.

tures was that by Kennedy and Murley[1]. Their computation shows a strong current crowding in these contacts. A different approach (Transmission Line Model) independently made by Berger[2] and by Murrmann and Widmann[3–5] led to qualitatively the same main result. However, due to the different basic assumptions, quantitatively as well as in other details, large differences occurred.

Although there has been some evidence[2, 3, 5] that the Kennedy–Murley Model does not adequately describe the usual aluminum–silicon contacts due to the disregard of interface resistance, a clear criterion for the applicability of one or the other model has been missing. Furthermore, some other questions mainly pertaining to a variety of operation conditions remained unanswered.

This paper gives a more extensive discussion of the planar contact. After an introduction of the basic assumptions underlying the different models, the Transmission Line Model (TLM) will be described, including the alternating current operation. Then experimental validity checks will be shown. An extension of the TLM, as it also allows the TLM to match the Kennedy–Murley conditions approximately, will define the validity ranges of the models and confirm the experimental findings. A discussion of the planar contact under different operation conditions concludes the paper.

2. BASIC CLASSIFICATION OF PLANAR CONTACTS

According to the direction of current flow in the semiconductor near the planar contact, two basic types of planar contacts are imaginable: the horizontal and the vertical type. For better illustration, a cross section of a common bipolar transistor is shown in Fig. 1. Near the base contact region the main current most likely flows horizontally, which leads to a current crowding at the contact edge. This characterizes the horizontal type. At the collector contact, however, the current would be expected to flow mainly vertically in a rather uniform distribution, due to the low-ohmic subcollector. Thus the collector contact would represent the vertical type. At low current levels, the emitter contact likely belongs to this category too; however, at high current levels the minority carrier injection is pushed to the emitter edges and then the contact probably becomes the horizontal type.

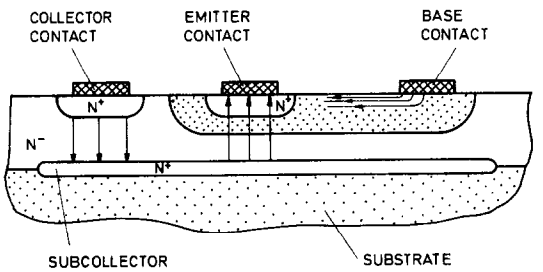

Fig. 1. Cross section through a planar *NPN* transistor with main current flow indicated by arrows.

With the contact resistivity ρ_c ($\Omega\,\mathrm{cm}^2$) as defined below [equation (2)], the contact resistance R_{cv} of a pure vertical type can easily be calculated using the equation

$$R_{cv} = \rho_c / A_c \quad (A_c = \text{contact area}). \tag{1}$$

The more difficult horizontal type and its models are the sole subject of discussion in this paper. The contacts on a diffused resistor appear to be the simplest and best representatives of the horizontal type and shall, therefore, be used in the analysis. The above mentioned base contact of a vertical *NPN* transistor, emitter and collector contacts of lateral bipolar transistors as well as source and drain contacts of field effect transistors can be expected to be further samples of the horizontal type of contact.

3. MODELS FOR THE HORIZONTAL TYPE OF PLANAR CONTACT

The subdivision of the contact region into the following main parts is assumed to reflect the reality well* [compare Fig. 2(a)].

- Semiconductor layer with a steep concentration gradient of the diffused impurity atoms
- High-ohmic interface layer
- Contact metal.

The terms by which these parts are usually characterized are well known. For the diffused layer these are the sheet resistance $R_s(\Omega/\square)$ and the junction depth X_j (or the diffusion length L), both in conjunction with the type of profile (complementary error function or gaussian).

*There are procedures for contact making, which result in a larger number of different layers than listed above; however, for the most common aluminum-silicon contact the list is considered sufficient.

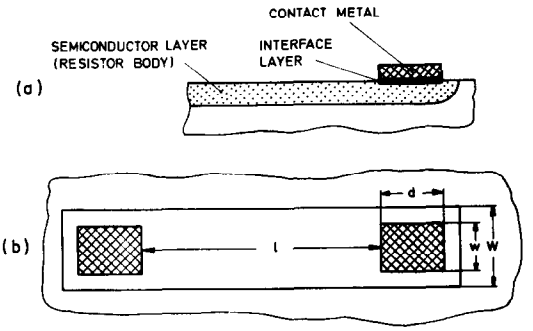

Fig. 2. Diffused resistor (a) cross section (b) top view.

Interface layers usually are characterized by the contact resistivity ρ_c:

$$\rho_c = \frac{v_c}{j_c} \quad \begin{matrix} (v_c = \text{voltage across the layer}) \\ (j_c = \text{current density there}). \end{matrix} \qquad (2)$$

The basic mechanisms which cause interface resistance and those which determine its amount are qualitatively well understood (see e.g. the contributions in [6]). Differences in work functions of metal and semiconductor, and surface states may lead to a depletion layer at the semiconductor surface. Electric current can surmount it by thermionic emission or by tunneling. For both mechanisms a voltage drop is required to obtain a net current. A thin layer of foreign matter—if present between metal and semiconductor—also requires a voltage drop to obtain a tunneling current. Sufficiently accurate quantitative predictions of the voltage-current density function of such metal-semiconductor interfaces have not been generally possible yet. This is especially true for the depletion layers of highly doped semiconductors typically present in ohmic contacts. Therefore, the interface still is preferably described by the lump sum 'contact resistivity', which is to be determined experimentally. One has to observe, however, that the defining equation (2) requires an ohmic behaviour of the interface and a current flow vertically to it. Although the current flow mechanisms of the interface usually lead to more or less non linear characteristics, these can be approximated by a linear one within a range of sufficiently small voltages v_c. Measurements by Ting and Chen [7] on typical contacts on highly doped silicon (surface doping $\geqslant 3 \times 10^{19}$ cm^{-3}) have shown good linearity up to at least a few 10 mV of interface voltage. This covers well the usual contact stresses. These results are confirmed by the author's measurements (Table 1). The required vertical current flow is approximately guaranteed even for the adverse geometry of a typical horizontal contact due to the high resistivity of the interface compared with that (ρ_B) of the undisturbed part of the semiconductor beneath. For example ρ_c-determinations using the TLM* as well as the measurements by Ting and Chen yield ratios $\rho_c/\rho_B > 10^{-4}$ cm in the typical surface doping range. The average resistivity ρ of the interface layer having a typical thickness of 10–100 Å would then be $\rho > 10^2$–$10^3\,\rho_B$.

The contact metal can also be characterized by its sheet resistance R_s; however, as this usually lies at least 2 orders of magnitude below that of the semiconductor, the metal will be considered a constant potential plane in the following.

In Fig. 3 the basic approximations made by Kennedy and Murley [1] on one side and those by Berger [2] and Murrmann and Widmann [3–5] on the other side are indicated and compared with reality. The two different approximations may be considered as extremes of the reality. Hence, they shall be called KM-extreme (after Kennedy and Murley) and TL-extreme (since it leads to the TLM). In the KM-extreme the interface resistance vanishes ($\rho_c \to 0$), but the semi-

*To be published elsewhere.

Table 1. Contact parameters of typical aluminum-silicon contacts in monolithic circuits according to the measurements in Figs. 7, 8 and 9

	1	2	3	4	5	6	7	8	9
Contact on	R_s ($\Omega/\square$)	ρ_c (Ω cm^2)	α [(μm)$^{-1}$]	$w \cdot Z$ (Ω cm)	$w \cdot R_c$ (KMM)* (Ω cm)	L_{Gaussian} (μm)	h_{eff}* (μm)	$\eta(h_{\text{eff}}$*)	5% linearity up to (mV)
Base	176	$1{\cdot}2 \times 10^{-5}$	0·38	$4{\cdot}7 \times 10^{-2}$	$1{\cdot}5 \times 10^{-2}$	0·9	1·7	2·4	100
Isolation	2·33	$6{\cdot}9 \times 10^{-7}$	0·18	$1{\cdot}25 \times 10^{-3}$	$6{\cdot}5 \times 10^{-4}$	2·2	5·6	1	25
Emitter	5·23	$2{\cdot}8 \times 10^{-7}$	0·43	$1{\cdot}2 \times 10^{-3}$	$2{\cdot}4 \times 10^{-4}$	0·5	0·9	7	20

*Profile measurements on these diffused layers showed a rather uniform carrier concentration down to some depth before the rapid fall-off started. Therefore, it appeared reasonable to approximate them by homogeneously doped layers of thickness h_{eff} rather than to use the theoretical gaussian profiles with the diffusion length L. This improved the KMM-figures of R_c (column 5) by about a factor of 2.

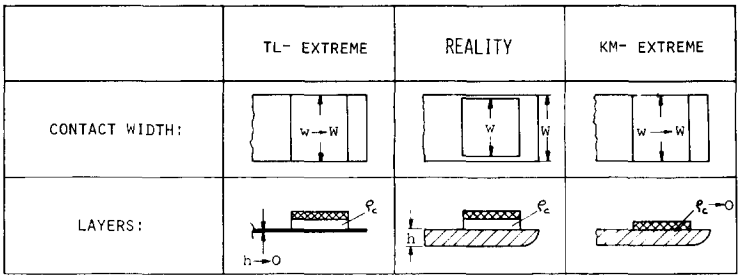

Fig. 3. Comparison of TL- and KM-approximation with reality.

conductor layer has a finite thickness h.* In the TL-extreme just this thickness becomes zero ($h \to 0$), but the layer retains its sheet resistance R_s. As the top views in Fig. 3 show, both for the TL- and the KM-extreme, the contacts are assumed as wide as the resistor†, which also departs from reality, where for tolerance reasons usually $w < W$ is maintained.

To arrive at a conclusion as to which approximation (KM or TL) is more realistic, experimental data and some more considerations are necessary, which will emanate from the TL-extreme.

4. THE TRANSMISSION LINE MODEL (TLM)

The TLM for the horizontal type of planar contact has been proposed independently by Berger[2] and by Murrmann and Widmann[3–5]. The latter started with the differential equations for the TL-extreme and took special solutions for the conditions of interest. Because of the identity of these differential equations with those of a transmission line, Berger directly started with more general solutions, the well known transmission line equations (5) and (6). Although this difference is subtle, the use of the transmission line equations as a general solution for the steady state facilitates the insight into the contact behaviour.

In Fig. 4 a cross section of a contact in the TL-extreme is compared with a transmission line section. To include the a.c.-operation, shunt capacitances are also drawn in the equivalent circuit of the line. This comparison tells that the resistance of the semiconductor layer corresponds to the series resistance R' of the transmission line, and that the interface resistance is the counterpart of the parallel shunt line conductance G'. Finally, the contact metal corresponds to the return lead. In the transmission line no series inductance has been considered, since a simple estimate tells that

*The current distribution calculations by Overmeyer [8] for homogeneous resistive layers having metal contacts also correspond to the KM-extreme, but are not directly aimed to contacts on semiconductors.

†In the case of KM-extreme this seems not to do justice to Kennedy and Murley, who included contacts with $w < W$ in their computation. However, this was not truly three-dimensional either.

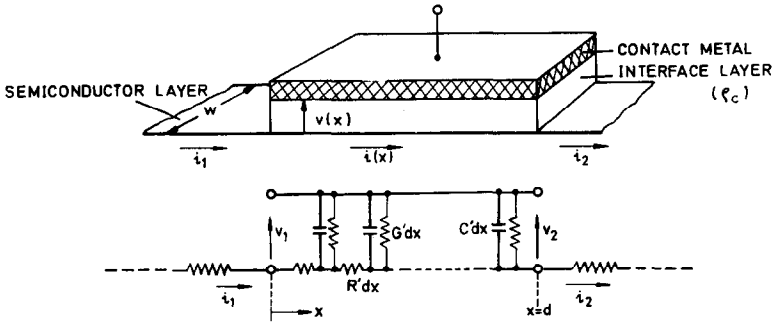

Fig. 4. Comparison of the contact region (TL-extreme) with a transmission line.

in the contact the inductance may be neglected as compared with the series resistance, even at extremely high frequencies.

Thus for the transmission line model of the contact region, the following equations of the primary line parameters can be written by comparison

$$R' = \frac{R_s}{w} \tag{3}$$

$$\underline{G}' = \frac{w}{\rho_c} + \mathcal{J}\omega \cdot wC^* = w\left(\frac{1}{\rho_c} + \mathcal{J}\omega C^*\right) \tag{4}$$

(C^* = capacitance per unit area).

The well known line equations (see e.g. [12]) then describe the current and voltage distribution along the contact according to Fig. 4:

$$\underline{V}(x) = \underline{V}_1 \cosh \gamma x - \underline{I}_1 \cdot \underline{Z} \sinh \gamma x \tag{5}$$

$$\underline{I}(x) = \underline{I}_1 \cosh \gamma x - \underline{V}_1/\underline{Z} \sinh \gamma x. \tag{6}$$

In these equations the secondary line parameters, known as characteristic impedance Z and propagation constant γ are [compare equations (3), (4)]:

$$\underline{Z} = \sqrt{\left(\frac{R'}{\underline{G}'}\right)} = \frac{1}{w}\sqrt{(R_s \cdot \rho_c)} \cdot \frac{1}{\sqrt{(1 + \mathcal{J}\omega C^* \cdot \rho_c)}} \tag{7}$$

$$\gamma = \alpha + \mathcal{J}\beta = \sqrt{(R' \cdot \underline{G}')} = \sqrt{\left(\frac{R_s}{\rho_c}\right)} \cdot \sqrt{(1 + \mathcal{J}\omega C^* \rho_c)}. \tag{8}$$

Now a normalized frequency is introduced:

$$\Omega = \frac{\omega}{\omega_c}, \tag{9}$$

$$\omega_c = (C^* \cdot \rho_c)^{-1}. \tag{10}$$

Since the d.c.-value of the characteristic impedance becomes

$$Z = \frac{1}{w}\sqrt{(R_s \cdot \rho_c)}, \tag{11}$$

and that of the propagation constant (which then is a pure attenuation constant)

$$\alpha_0 = \sqrt{\left(\frac{R_s}{\rho_c}\right)}, \tag{12}$$

equations (7) and (8) can be simply written as

$$\underline{Z} = \frac{Z}{\sqrt{(1 + \mathcal{J}\Omega)}} \tag{13}$$

and

$$\gamma = \alpha_0\sqrt{(1 + \mathcal{J}\Omega)}. \tag{14}$$

Whether the frequency dependence of the contact has to be considered depends on the cut-off-frequency ω_c [equation (10)]. By estimating C^*, taking the silicon lattice constant (≈ 5 Å) as an absolute minimum for the depletion layer thickness and by using experimentally determined ρ_c-values, this frequency has been found to lie at least in the range of GHz for typical aluminum-silicon contacts. Therefore, for these the frequency dependence usually need not be considered. This might not be true for other metal–semiconductor pairs.

For the most important d.c.-case the line equations (5) and (6) become

$$v(x) = v_1 \cosh \alpha x - i_1 \cdot Z \sinh \alpha x \tag{15}$$

$$i(x) = i_1 \cosh \alpha x - v_1/Z \sinh \alpha x \tag{16}$$

(x = distance from the leading contact edge, compare Fig. 4. The index of α_0 has been omitted for simplicity).

From these equations all questions pertaining to the currents, current densities and voltages as well as to their quotients (resistance values) can be answered. Before this will be done in more detail, basic conclusions for experimental validity checks of the model will be discussed.

5. EXPERIMENTS

To check whether the model is valid in spite of the approximations used (Fig. 3), it is reasonable to compare measurements with theoretical conclusions from the model. However, adequate data on contact resistivity ρ_c to be inserted in the model are missing. It does not seem reasonable to extrapolate from the few data reported in the literature (e.g. [9]) to the diffused resistor structures at hand, mainly as the difference in contact area is very large (ratio $> 10^4$) and as the dependence on process differences and semiconductor surface doping might be too strong. Theoretical predictions are even less useful at present*.

*Compare the small print remarks in Section 3.

The second unknown, the sheet resistance R_s of the semiconductor layer beneath the contact metal, can be easily determined as long as it remains identical with that of the original resistor diffusion. However, one can imagine that the latter might be changed by the contact making process. This is evident for Mo–PtSi–Si contacts, where the PtSi forms a relatively low-ohmic layer. Chang's measurements[11] indicate, that the TLM is applicable to this contact type, if the changed sheet resistance is considered. Even on his Al–Si contacts Chang found, that they could be satisfactorily described only by assuming a severe lowering of sheet resistance, although there is no evident physical background in this case. The author's measurements on Al–Si contacts as presented below do not confirm this Chang's observation. Rather an undisturbed sheet resistance has been profitably assumed throughout the evaluation of the measurement results.

Instead of assuming a certain contact resistivity beforehand, the model can be checked via the contact length dependences and the interdependences of measurable contact features. Two terms seem useful for this purpose, the contact resistance R_c and the contact end resistance R_e. It is convenient to refer contact resistance to the end correction term k usually used for calculating the total resistance R_{tot} of a monolithic resistor (compare Fig. 2)

$$R_{tot} = R_s\left(\frac{l}{W} + 2k\right). \tag{17}$$

by setting

$$R_c = R_s \cdot k \tag{18}$$

so that

$$R_{tot} = R_s \cdot \frac{l}{W} + 2R_c. \tag{19}$$

With these equations the hypothetical separation between resistor body and contact region is made directly at the inner contact edge*. Therefore, in case of $w = W$ (compare Fig. 2) the contact resistance becomes equal to the input resistance of the TLM-two-port Fig. 4:

$$R_c = \frac{v_1}{i_1} \tag{20}$$

With $i(d) = i_2 = 0$ (compare Fig. 4) R_c then is according to equation (16)

$$R_c = \left.\frac{v_1}{i_1}\right|_{i_2=0} = Z \coth \alpha d. \tag{21}$$

Hence, with increasing contact length d, the contact resistance approaches asymptotically to Z. Already with $\alpha d = 1{\cdot}5$, R_c deviates from Z only by 10 per cent.

For the usual case ($w < W$) equation (21) only approximates the actual contact resistance, as the TLM besides its other inherent approximation ($h \to 0$) does not consider the non-uniform current spread around the contact present with $w < W$. As will be shown in Section 7, the error very likely is small for practical purposes.

A resistor structure with three equal contacts in different distances as depicted in Fig. 5 allows to determine R_c according to equation (19). This equation, when applied to the separately measured resistance values R_1 and R_2, leads to

$$R_c = \frac{R_2 \cdot l_1 - R_1 \cdot l_2}{2(l_1 - l_2)}. \tag{22}$$

It should be noted that equations (17) and (18) make practical sense only as long as k or R_c are independent on the contact distance l. Or in other words, the current distribution near a contact must not be noticeably influenced by the other contact. With the usual designs ($w < W$) it requires a minimum distance between the

*A more general definition of contact resistance is possible and will be published elsewhere.

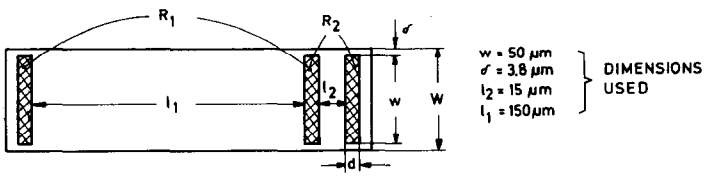

Fig. 5. Resistor test structure for determination of contact resistance R_c and contact end resistance R_e.

contacts. In the design of diffused resistors this requirement is usually considered and must be observed, of course, also in case of the test structure Fig. 5 to render equation (22) valid as well as equation (26) below.

R_c-measurements on aluminum–silicon contacts of a typical monolithic process have shown that even near the minimal contact length ($\approx 4\ \mu$m) R_c does not decrease substantially when the contact is prolonged. The small decrease almost vanishes in the measurement error. Therefore, a quantitative comparison with the model is difficult, although qualitatively the contacts behave as expected.

A better means of comparison is the contact end resistance R_e. This term has been defined[2] as voltage drop $v_2 = v(d)$ at the end of the contact divided by the input current i_1 for $i_2 = 0$ (compare Figs. 4 and 6):

$$R_e = \left.\frac{v_2}{i_1}\right|_{i_2=0}. \tag{23}$$

From the line equations (15), (16) this term becomes

$$R_e = \frac{Z}{\sinh \alpha d}. \tag{24}$$

Equation (21) tells, that Z can be determined from R_c for long contacts ($\alpha d \geq 2$). The attenuation constant is according to equations (11) and (12)

$$\alpha = \frac{R_s}{w \cdot Z}. \tag{25}$$

R_s can be calculated from R_1 and R_2 of the structure in Fig. 5, if one assumes that the semiconductor sheet resistance beneath the contact metal equals that of the resistor body:

$$R_s = (R_1 - R_2) \cdot \frac{W}{l_1 - l_2}. \tag{26}$$

Figures 7–9 show the measured contact end resistances vs. contact length for three different contact types (aluminum on base diffusion, isolation diffusion and emitter diffusion). The full lines indicate the theoretical curves calculated from the measured R_s and $R_c \approx Z$ of long contacts, using equations (25) and (24). Table 1 lists all measured or calculated parameters. For the base diffused silicon case (Fig. 7) the agreement with the model is satisfactory. The isolation diffused case (Fig. 8) allowed a comparison also of the

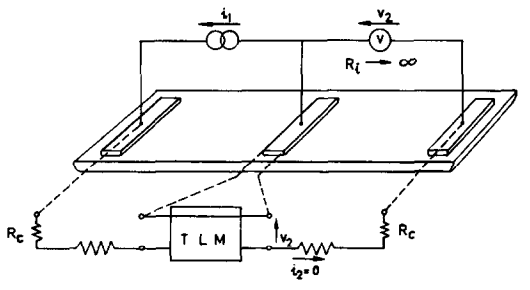

Fig. 6. Measurement of contact end resistance R_e according to equation (23).

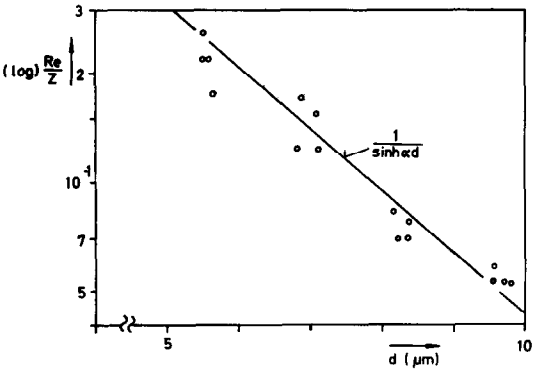

Fig. 7. Measured contact end resistance R_e vs. contact length d for aluminum contacts on base diffused silicon, compared with TLM-prediction. (Estimated maximum errors: $\Delta d \approx \pm 0{\cdot}3\ \mu$m, $\Delta R_e/R_e \approx \pm 0{\cdot}5\%$).

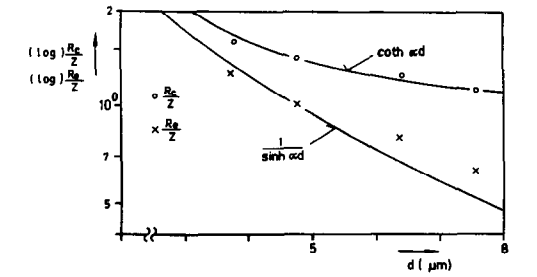

Fig. 8. Measured contact resistance R_c and contact end resistance R_e vs. contact length d for aluminum contacts on isolation diffused silicon, compared with TLM-prediction (only average values because of small scattering of results; estimated maximum error: $\Delta d \approx \pm 0{\cdot}3\ \mu$m, $\Delta R_c/R_e \approx \pm 5\%$, $\Delta R_e/R_e \approx \pm 0{\cdot}5\%$).

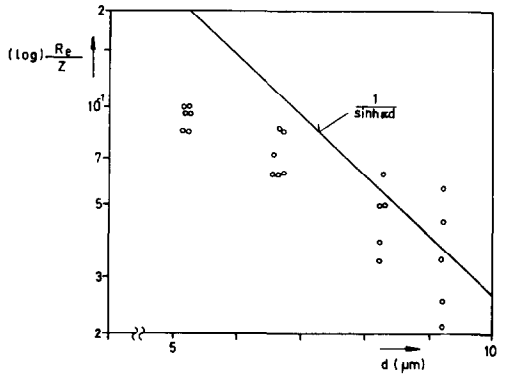

Fig. 9. Measured contact end resistance R_e vs. contact length d for aluminum contacts on emitter diffused silicon, compared with TLM-prediction. (Estimated maximum error: $\Delta d \approx \pm 0{\cdot}3\ \mu m$, $\Delta R_e/R_e \approx \pm 0{\cdot}5\%$).

R_c-values, since there the contact length dependence was just large enough. A good coincidence is found here too. Only the contacts on emitter diffused regions behaved somewhat erratic (Fig. 9). A closer inspection revealed that these contacts were very non-uniform. Of course, in this case the model cannot apply well. But still, the general trend is satisfactory. In total the measurements show that the TLM is a useful approach*.

The rule of thumb of Kennedy and Murley[1] $R_c \approx 0{\cdot}5R_sL/W$ (L = diffusion length of dopant atoms) predicts contact resistances smaller at least by a factor of 2 than obtained in the measurements above, even if a larger term 'h_{eff}' is used instead of L (compare columns 4–7 and the footnote of Table 1). This indicates that the interface resistance may not be neglected at least in case of these typical aluminum–silicon contacts. A more general statement will result from the following considerations.

6. THE EXTENDED TLM (ETLM)

Although the TLM has proven itself satisfactory for the most important aluminum–silicon contacts, an inclusion of the vertical resistance of the semiconductor layer would increase the confidence in the model for application also to other metal semiconductor pairs.

For this purpose a contact on a homogeneously doped semiconductor layer of bulk resistivity ρ_B shall be considered first. As indicated in Fig. 10 the addition of a part $C \leqslant 1$ of the vertical semiconductor resistance of a unit area $\rho_B \cdot h$ to the contact resistivity shall approximately account for the vertical voltage drop in the semiconductor layer. With this supposition an apparent contact resistivity ρ_c^* can be defined by

$$\rho_c^* = \rho_c + C \cdot \rho_B \cdot h. \tag{27}$$

Inserting this apparent contact resistivity into equation (12) instead of using the actual one, one obtains the new attenuation constant

$$\alpha^* = \frac{1}{\sqrt{(\eta + C)}} \cdot \frac{1}{h}, \tag{28}$$

where the relation

$$R_s = \frac{\rho_B}{h} \tag{29}$$

and the abbreviation

$$\eta = \frac{\rho_c}{\rho_B \cdot h} \tag{30}$$

have been used.

Accordingly, using equations (11) and (12) one obtains the new characteristic contact resistance

$$Z^* = R_s \cdot \frac{h}{w} \sqrt{(\eta + C)}\,. \tag{31}$$

The term η can be interpreted as the ratio of the contact interface resistance to the vertical semiconductor resistance in a prism cut out vertically to the contact plane. Hence it is imaginable that it predicates the relative influence of the contact interface on one side and of the vertical extension and resistivity of the semiconductor layer on the other side on the current spreading in the contact

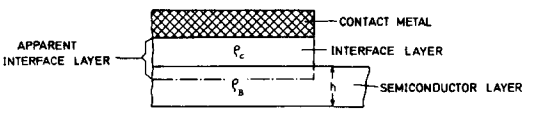

Fig. 10. Extension of the TLM by defining an apparent interface layer.

*Murrmann and Widmann[5] also obtained a satisfactory agreement of measured $R_e = f(d)$ with the TLM for an Al-contact on a base diffused resistor.

region. Concurrently with this consideration, the KM-extreme in which the interface resistance is neglected ($\rho_c = 0$, $\eta = 0$) can be characterized for practical purposes by $\eta \ll C$ according to equations (28) and (31). Vice versa, the TL-extreme where the vertical extension of the semiconductor layer is neglected ($h \to 0$, $\eta \to \infty$) practically means $\eta \gg C$.

A reasonable value for C can be found by comparison of the characteristic resistance Z^* with results of Ting and Chen[7]. By conformal mapping they have determined the contact resistance of an infinitely long contact on an homogeneous layer at the KM-extreme:

$$R_c|_{KM} = R_s \cdot \frac{h}{w} \cdot \frac{\ln 4}{\pi}. \tag{32}$$

The comparison with equation (31) immediately tells ($\eta = 0$):

$$C = \left(\frac{\ln 4}{\pi}\right)^2 = 0{\cdot}19. \tag{33}$$

Overmeyer[8] has shown that at the KM-extreme the current distribution over the contact length is almost identical for a homogeneous layer and a diffused layer, if one sets $h = L$. (L = Diffusion length of the dopant.) Indeed, if one takes the KM-rule of thumb[1] $R_c \approx 0{\cdot}5R_sL/W$ the comparison with equation (31) then yields $C \approx 0{\cdot}23$ which is close to the value obtained for the homogeneous layer. Thus 0·2 would be a good number for C and can be easily retained.

Model measurements ($\eta = 0{\cdot}7$ and $\eta = 1{\cdot}5$) have shown that the extension of the TLM by the apparent contact resistivity and $C \approx 0{\cdot}2$ is indeed a satisfactory approximation for practical purposes. Also the theoretical comparison of the current distribution for $\eta = 0$ on the basis of Overmeyer's calculations[8] proves satisfactory (see Fig. 11).

The changeover from the TLM to the ETLM basically means a new and more general interpretation of the parallel shunt conductance [equation (4)] of the transmission line, where now the *apparent* contact resistivity is assumed determining. Since in the measurement evaluations of the foregoing section the contact resistivities have been indirectly determined via the TLM, these values (column 2 of Table 1) should rather more generally be interpreted as apparent contact

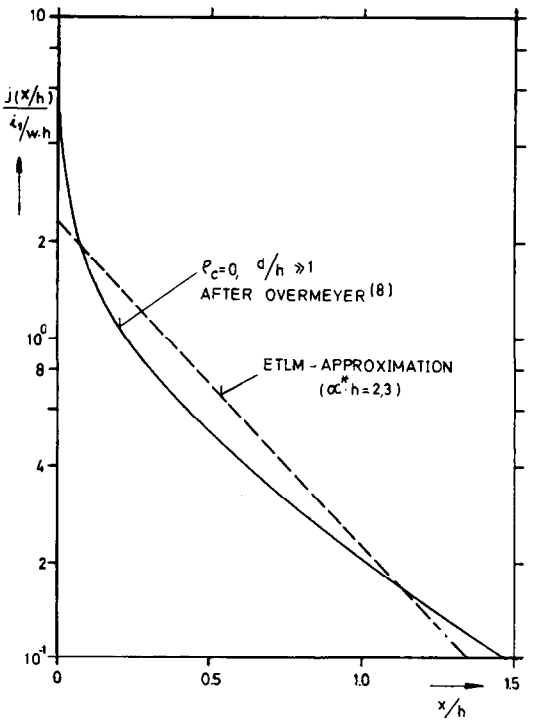

Fig. 11. Current distribution along a rectangular contact on a homogeneous resistance layer under KM-extreme (after Overmeyer), compared with the ETLM-approximation.

resistivities ρ_c^* of the ETLM.* A correction by about $-C/\eta \times 100$ per cent then yields the actual contact resistivity [compare equations (27) and (30)]. According to the calculated η (Table 1), the contact on isolation diffusion requires the largest correction of 20 per cent. For all three contact types η lies far away from the KM-extreme ($\eta \ll 0{\cdot}2$) which underlines that the KMM is indeed not applicable.

In total, the ETLM has yielded a criterion to determine, whether the KMM or the TLM is valid for a given contact, when contact resistivity and the semiconductor data are known. Further, the ETLM allows to approximately describe contacts even down to the KM-extreme, in a range where closed analytical expressions have not been available. It further tells, how to separate the actual contact resistivity from the apparent one determined via the ETLM.

*The calculated α and the measured Z accordingly should be interpreted as pertaining to the ETLM (α^*, Z^*) as well.

7. THE EFFECT OF THE CONTACT WIDTH APPROXIMATION

So far it has been shown that one of the TLM-approximation errors, the infinitely thin semiconductor layer, can be lessened by using the ETLM. The other approximation error, namely assuming that the contact extends over the total resistor width ($w = W$), is not as easy to resolve but does not appear severe either with typical contacts.

The problem is illustrated in Fig. 13, where a sketch of the current lines is given for a contact region with $w < W$. In the semiconductor layer outside the contact the resistance is increased when compared with a contact of $w = W$, due to the lateral current crowding. For reference purposes this effect shall be designated as lateral effect. Contrary to the latter contribution, the now ($w < W$) partly utilized contact sides might reduce the transition resistance between metal and semiconductor as compared to a contact of the same width but with $w = W$. This shall be referred to as gap effect.

The lateral crowding resistance for a sufficiently long contact can be roughly estimated* by assuming a contact with zero contact resistivity on an extremely thin semiconductor layer, thus reducing the problem to a two-dimensional one.

Ting and Chen[7] have calculated this lateral crowding resistance R_l by conformal mapping. Their result can be written in the form

$$\frac{R_l}{Z}\cdot\frac{1}{\alpha}=\frac{w}{2\pi}\left(\frac{1}{K}\ln\frac{K+1}{K-1}-\ln\frac{K^2}{K^2-1}\right) \qquad (34)$$

with $K = (w+2\delta)/2\delta$ (compare Fig. 13).

Since δ is predetermined by mask alignment and etching tolerances, it seems reasonable to plot curves of constant δ and variable w, as shown in Fig. 13. E.g. with a typical $\alpha \approx 0{\cdot}4/\mu m$ and $\delta = 2{\cdot}5$ μm the peak error of the TLM would be estimated to 8 per cent. Measurements by d'Andrea and Murrmann[10] on various contact configurations seem to indicate that the actual influence of the lateral effect on the contact resistance is smaller than the estimate of equation (34) or even is covered by other influences.

*Strictly speaking, both the lateral and the gap effect in general cannot be calculated separately, since the contact features are a boundary condition for the lateral current distribution and vice versa, the lateral current distribution affects the transition resistance of the contact.

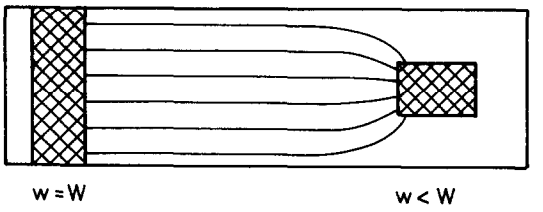

Fig. 12. Sketch of lateral current crowding at a contact $w < W$.

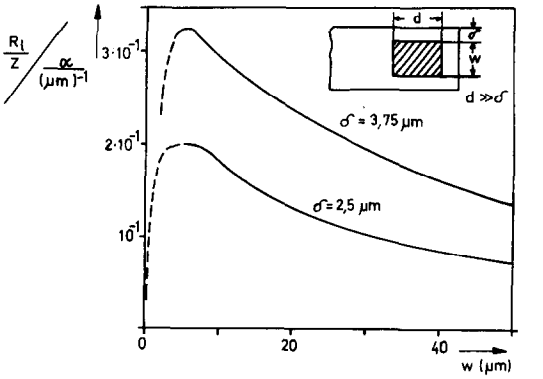

Fig. 13. Normalized lateral crowding resistance as a function of contact width w for fixed distances δ (contact edge ↔ resistor edge).

Chang[11] has suggested to approximately consider the gap effect alone by shunting the series resistance of the TLM by that of the two δ-wide gaps between resistor and contact side edges. According to his measurements on 58 μm wide resistors this modification becomes significant for gaps $\delta \geq 15\,\mu m$ and fits satisfactorily to the data. However, since usual fabrication tolerances allow for $\delta \leq 4$ μm, the modification does not appear necessary for practical structures of this resistor width and contact type.

Again from a practical viewpoint, measurements on contacts of various widths but constant δ would be very helpful to gain a better insight into the relative significance of the lateral and the gap effects. Such measurements are not available yet. However, all the other data indicate, that the accuracy of the TLM for usual contacts with $w < W$ is sufficient.

8. CONCLUSIONS FROM THE TLM

Above it has been shown that the TLM, or where necessary, the ETLM is a useful approach

to describe planar contacts of the horizontal type. Therefore, it is worthwhile to draw some conclusions from the TLM for the contact behaviour under various conditions. Some of them have been presented already in[2–5]. For the sake of completeness they shall be included here.

For the TLM two-port shown in Fig. 6 in the special operation mode $i_2 = 0$, more generally any value of i_2 is possible. The contacts shall be classified after their operation mode:

(1) $i_1 \neq 0$, $i_2 = 0$ terminal contact

(2) $i_1 \neq 0$, $i_2 \neq 0$ intermediate contact

(a) $i_1 = i_2$ symmetrical supply contact*

(b) $i_1 = -i_2$ unloaded tap

The designations have been chosen according to the prevailing function or geometrical arrangement of the contacts in those operation modes.

The simplest case is the terminal contact. The contact resistance for this type has been given already by equation (21). Using equations (11) and (12) it can be written as

$$R_c = R_{cv} \cdot \alpha d \coth \alpha d \tag{35}$$

with

$$R_{cv} = \frac{\rho_c}{w \cdot d}, \tag{36}$$

which is the contact resistance for a contact with uniform current distribution ['vertical planar contact' compare equation (1)]. Depending on the value of αd the following approximations for R_c can then be derived (error smaller than 10 per cent):

$$R_c \approx R_{cv} = \frac{\rho_c}{w \cdot d} \qquad (0 \leq \alpha d \leq 0{\cdot}5), \tag{37}$$

$$R_c \approx R_{cv} + \frac{1}{3} R_{ss} \qquad (0 \leq \alpha d \leq 1{\cdot}5), \tag{38}$$

*An example for this contact type most likely is the base contact between two emitter stripes of a bipolar transistor.

where

$$R_{ss} = R_s \cdot \frac{d^*}{w}. \tag{39}$$

Finally

$$R_c \approx Z = \sqrt{(R_{cv} \cdot R_{ss})} (1{\cdot}5 \leq \alpha d < \infty). \tag{40}$$

These approximations provide a relation between the contact resistances of the horizontal and the vertical planar contact.

The current density in the contact area is according to equation (2)

$$j(x) = \frac{v(x)}{\rho_c}. \tag{41}$$

From the line equations (15) and (16) follows with the condition $i_2 = 0$:

$$v(x) = i_1 \cdot Z \cdot \frac{\cosh [\alpha d(1 - x/d)]}{\sinh \alpha d}. \tag{42}$$

With equations (41), (11) and (12) it can be written as

$$\frac{j(x)}{\bar{j}} = \alpha d \frac{\cosh [\alpha d(1 - x/d)]}{\sinh \alpha d}, \tag{43}$$

where $\bar{j} = i_1/wd$ is the average current density in the contact area. Figure 14 shows the current distribution over the relative distance from the leading contact edge for various αd-values. The peak current density, of course, occurs at the leading contact edge ($x = 0$) and has the value [equation (43)]

$$\hat{j} = \frac{i_1}{w} \cdot \alpha \cdot \coth \alpha d. \tag{44}$$

That means, it depends on the contact length d the same way as the contact resistance (see Fig. 15). For a sufficiently long contact ($d \geq 1{\cdot}5/\alpha$) both the contact resistance and the peak current density cannot anymore be diminished appreciably by contact prolongation. There exists a final value for both. Since $\hat{j}$ increases with α, and since the KMM ($\eta \to 0$) yields the largest α [compare equation (28)], the KMM usually predicts pessimistic current density values.

*Thus R_{ss} is the total series resistance of the semiconductor beneath the contact.

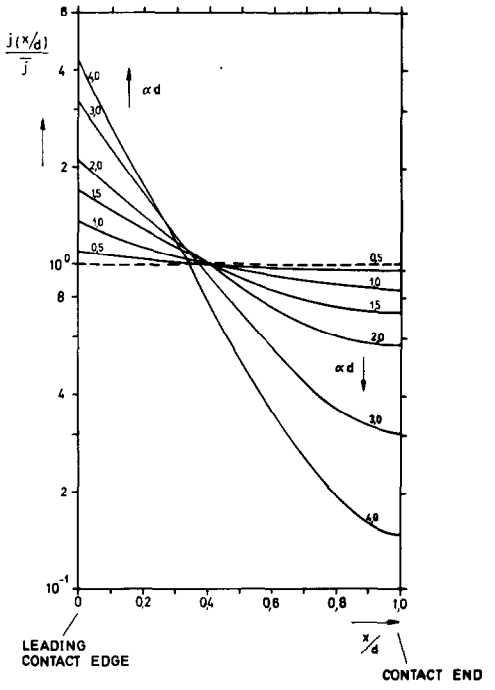

Fig. 14. Current distribution along a rectangular horizontal planar contact, αd = parameter.

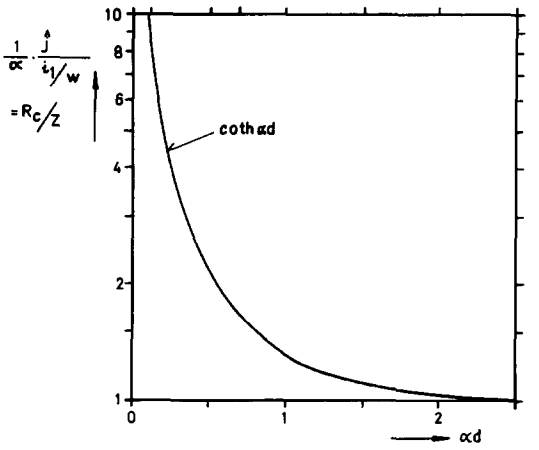

Fig. 15. Normalized peak current density j or normalized contact resistance R_c as a function of normalized contact length d.

Contact resistance and current density of the intermediate contact can be derived most easily from the terminal contact by linear superposition of the current-voltage distributions caused separately by i_1 and i_2.

For the contact resistance this leads to

$$R_{ci} = R_{ct} + R_e \cdot \frac{i_2}{i_1}. \tag{45}$$

where R_{ct} and R_e refer to the terminal contact. $|i_2/i_1|$ is unity for the symmetrical supply contact and for the unloaded tap. Thus their contact resistances differ from that of the terminal contact (R_{ct}) by just a contact end resistance (R_e).

The superposition of the current densities results in [compare equation (43)]

$$\frac{j(x)}{\bar{j}_1} = \frac{\alpha d}{\sinh \alpha d}\left\{\cosh\left[\alpha d\left(1-\frac{x}{d}\right)\right] + \frac{i_2}{i_1}\cosh \alpha x\right\}. \tag{46}$$

A contact type of interest not considered so far is the circular contact* with a radial current flow (e.g. the emitter contact of a circular *PNP* transistor or the source contact of a circular FET). By solving the differential equations for the here radially dependent line parameters R' and G', one obtains for the contact resistance

$$R_c = \frac{\sqrt{(R_s \cdot \rho_c)}}{\pi \cdot r_d} \cdot \frac{\mathcal{T}_0(\mathcal{J}\alpha r_d)}{2[-\mathcal{J}\mathcal{T}_1(\mathcal{J}\alpha r_d)]} \tag{47}$$

and for the current distribution

$$\frac{j(r)}{\bar{j}} = \alpha r_d \frac{\mathcal{T}_0(\mathcal{J}\alpha r)}{2[-\mathcal{J}\mathcal{T}_1(\mathcal{J}\alpha r_d)]} \tag{48}$$

(r = distance from the contact center)
(r_d = contact radius).

The quotient of the Besselfunctions occurring in equation (47) is shown in Fig. 16 with its approximations. Further a diagram for the current distribution has been drawn (Fig. 17) similar to Fig. 14. However, comparisons with the rectangular contact must consider that the circular contact has one degree of freedom less than the rectangular contact.

*Ring contacts are not considered here, since they usually have a radius r_d large enough so that they can be treated approximately as a rectangular contact of width $w = 2\pi r_d$ (see also the approximations by Murrmann and Widmann[4]).

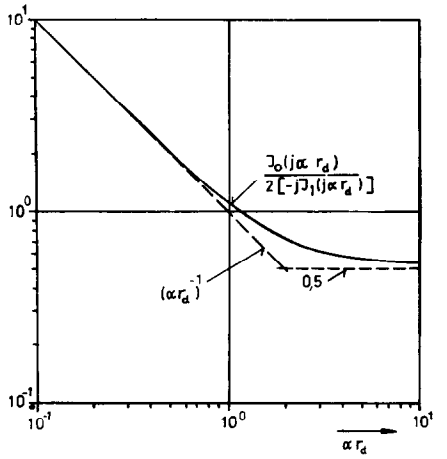

Fig. 16. Quotient of Besselfunctions pertaining to contact resistance R_c and peak current density $j = j(r_d)$ of a circular contact, and its approximations.

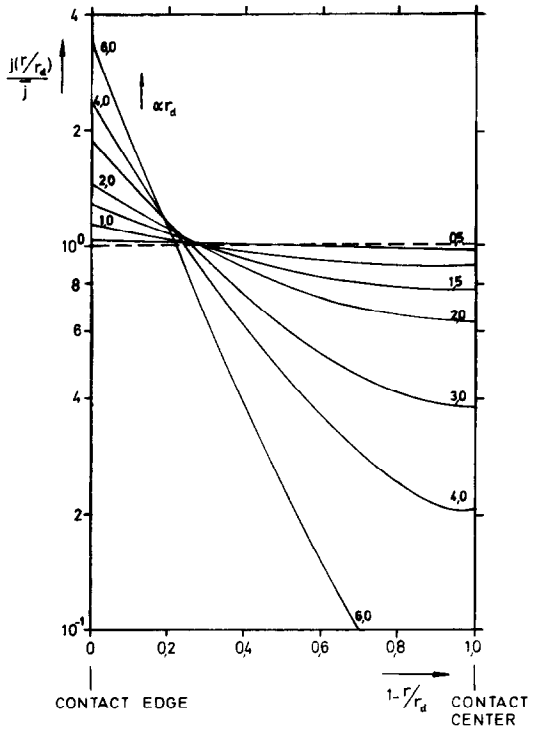

Fig. 17. Radial current distribution on a circular contact, αr_d = parameter.

9. SUMMARY AND CONCLUSIONS

In this paper a relationship between the two basic models (KMM and TLM) for the horizontal type of contacts to planar devices has been revealed via the extended TLM (ETLM). Namely, the ETLM-approximation provides a continuous transition from the KMM to the TLM, each one having its certain range of applicability.

The calibration of the ETLM on the KM-conditions, for which the work of Kennedy and Murley[1], Ting and Chen[7] and Overmeyer[8] has been used, has yielded a simple quantitative criterion for these ranges of applicability. This criterion weighs the relative influence of contact resistivity on one side and the resistivity and vertical structure of the semiconductor layer on the other side. According to the criterion and to measurement results, usual aluminum–silicon contacts follow the (E)TLM, but not the KMM.

The ETLM-transition established between KMM and TLM aids to realise, that both models must concurrently predict the non-uniform current distribution in the contact area and the relative insensitivity of contact resistance to contact prolongation, although with quantitatively quite different results.

From an engineering point of view, the (E)TLM-approximation (including $w < W$) appears to be sufficiently accurate for the treatment of at least the usual planar contacts. As has been shown in the last section, various operation conditions as well as circular contacts can be readily described.

A weak point in the application of the (E)TLM is the lack of sufficient data on contact resistivity vs. semiconductor surface doping for various contact metals. However, the TLM itself provides a new tool to gather such data and thus might also be able to promote the adjustment of theoretical predictions of contact resistivity.

REFERENCES

1. D. P. Kennedy and P. C. Murley, *IBM J. Res. Dev.* **12**, 242 (1968).
2. H. H. Berger, *Dig. Tech. Pap. ISSCC* p. 160 (1969).
3. H. Murrmann and D. Widmann, *Dig. Tech. Pap. ISSCC*, p. 162 (1969).
4. H. Murrmann and D. Widmann, *Solid-St. Electron.* **12**, 879 (1969).
5. H. Murrmann and D. Widmann, *IEEE Trans. Electron Devices*, **ED-16**, 1022 (1969).
6. B. Schwartz, *Ohmic Contacts to Semiconductors*, The Electrochemical Soc. (1969).

7. C. Y. Ting and C. Y. Chen, *Solid-St. Electron.* **14**, 433 (1971).
8. J. Overmeyer, *IBM J. Res. Dev.* **14**, 66 (1970).
9. R. C. Hooper, J. A. Cunningham and J. G. Harper, *Solid-St. Electron.* **8**, 831 (1965).
10. G. D'Andrea and H. Murrmann, *IEEE Trans. Electron Devices*, **ED-17**, 484 (1970).
11. I. R. Chang, *J. electrochem. Soc.* **117**, 368 (1970).
12. H. G. Unger, *Theorie der Leitungen*, Verlag F. Vieweg, Braunschweig (1967).